Green Chemistry

CRITICAL REVIEW

View Article Online
View Journal

Cite this: DOI: 10.1039/c9gc01806a

Are lignin-derived carbon fibers graphitic enough?

William J. Sagues,[a] Ankush Jain,[b] Dylan Brown,[a] Salonika Aggarwal,[a] Antonio Suarez,[a] Matthew Kollman,[a] Seonghyun Park[a] and Dimitris S. Argyropoulos *[a,c]

Received 31st May 2019,
Accepted 11th July 2019

DOI: 10.1039/c9gc01806a

rsc.li/greenchem

Single component lignin-derived carbon fibers have been under development for many years, but strength properties are still inferior to those of commercial carbon fibers. The extent of graphitization is an overlooked limitation to lignin-derived carbon fiber development, particularly for high-modulus fibers treated at high temperatures. The tensile moduli of commercial carbon fibers increase with temperature during graphitization, however, lignin-derived carbon fiber moduli stay the same or decrease. This review exposes the inability of lignin-derived carbon fibers to graphitize in a manner similar to commercial carbon fibers, thereby providing rationale for the aforementioned discrepancy in tensile moduli-temperature trends and offering possible tangible future areas of research and development.

Introduction

Commercial carbon fibers (CFs) are typically classified based on their tensile modulus, although other properties significantly influence performance. Low modulus carbon fibers (LMCFs) have modulus values typically under 350 GPa, whereas high modulus carbon fibers (HMCFs) have values above 350 GPa.[1] HMCFs are of high value due to their ability to reinforce lightweight composites in applications such as aviation and aerospace. Commercial HMCFs are often derived from polyacrylonitrile (PAN) and have excellent properties for high performance, high strength, lightweight materials. However, the PAN precursor is very expensive, accounting for 50% of the final CF product cost.[2] The high cost of PAN-derived CFs has encouraged researchers to look for inexpensive substitutes, such as lignins. Researchers have attempted to produce lignin-derived carbon fibers of two

[a]Department of Forest Biomaterials, North Carolina State University, 2820 Faucette Dr, Raleigh, NC 27606, USA. E-mail: dsargyro@ncsu.edu
[b]Department of Chemical & Biomolecular Engineering, North Carolina State University, 911 Partners Way, Raleigh, NC 27606, USA
[c]Department of Chemistry, North Carolina State University, 2700 Stinson Dr, Raleigh, NC 27607, USA

William "Joe" Sagues, Ankush Jain, Dylan Brown, Salonika Aggarwal, Antonio Suarez, Matt Kollman, and Seonghyun Park (from left to right)

This team of coauthors contributed to the paper as part of Dr Dimitris Argyropoulos' advanced course on lignocellulose conversion chemistry. Unless noted, all coauthors are affiliated with the Department of Forest Biomaterials at North Carolina State University. William "Joe" Sagues is a PhD student developing bio-based graphitic carbon materials for use in lithium-ion anodes. Ankush Jain is a MS student in the Department of Chemical & Biomolecular Engineering elucidating the mechanism for pyrolysis of hemicellulose. Dylan Brown is a MS student optimizing microbiological conversion of lignin to value added chemicals. Salonika Aggarwal is a PhD student researching supercritical CO_2 extraction of lignocellulose for value added composite materials. Antonio Suarez is a PhD student performing techno-economic assessments of biomass conversion processes. Matt Kollman is a PhD student studying chemical modification of lignin to increase its functionality as a macromonomer as well as the thermochemical conversion of lignin to liquid hydrocarbons. Seonghyun Park is a PhD student researching cellulose modification and associated derivatives.

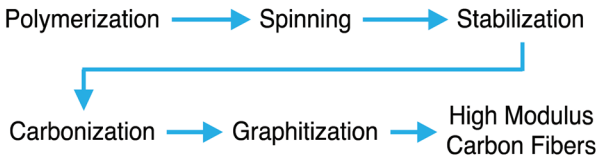

Fig. 1 Generalized process for the production of high modulus carbon fibers.

general classifications: (1) single component fibers in which lignin is the only precursor and (2) multi-component fibers in which lignin is blended with other polymers.

The manufacturing operations involved in the production of LMCFs and HMCFs are basically the same aside from downstream operations in which HMCFs undergo high temperature graphitization (2000–3000 °C), as shown in Fig. 1.[1] During graphitization, carbon fiber tensile modulus increases while tensile strength usually decreases.[3] The high tensile modulus associated with HMCFs, as well as the high structural rigidity and low coefficient of thermal expansion, are due in large part to the highly oriented, basal-plane-based graphitic crystallites that form along the fiber axes during high temperature treatment.[1] During graphitization of commercial HMCFs, disordered sp^3-hybridized polymeric clusters transition to ordered sp^2-hybdridized. This structural transition is clearly evident from X-ray diffraction (XRD) and Raman spectroscopy, as shown in Fig. 2A & B.[4] As the temperature increases, the peak width of the X-ray diffractogram and the I_D/I_G ratio of the Raman spectra decrease, indicating an increase in graphitic crystallite size (L), quantified by eqn (1) & (2)[5,6] and corroborated by Fig. 2C.[7] Graphite has a characteristic (002) peak at $2\theta = 26.7°$ *via* XRD, and therefore ordered materials containing highly graphitic crystallites will have a large, narrow peak at this angle with a flat baseline; jagged baselines and turbulent curves for carbon materials indicate disorder. Thus, the average graphite crystallite size in high quality, commercially produced HMCFs is relatively large and easily identifiable and quantifiable through XRD and Raman spectroscopy. Moreover, the presence of large graphite crystallites in CFs indicates the proper structural arrangement for high tensile modulus.[8] In this review, we present evidence for the lack of graphitic structure in lignin-derived carbon fibers through discussion and presentation of both qualitative and quantitative information obtained from numerous studies focused on carbon fibers and lignin carbonization; the majority of data presented is qualitative from XRD and Raman spectroscopy since graphitic structure can be easily detected and broadly assessed with such methods. Given the lack of robust data in the literature, we do not delve deeply into the effects of varying lignin types and other parameters such as lignin isolation method and carbonization time; we do however discuss the effects of temperature on graphitic structure development. The scope of this review is primarily confined to single-component lignin CFs to clearly illustrate the inability of lignin to graphitize in the same way as polymers used in commercial CF production.

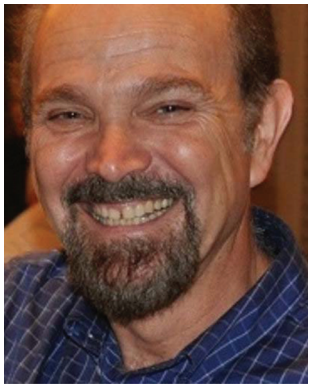

Dimitris S. Argyropoulos

Dr Argyropoulos is a Professor of Chemistry with the Departments of Chemistry and Forest Biomaterials at North Carolina State University (NCSU). Dr. Argyropoulos has served as a PAPRICAN (Pulp & Paper Research Institute of Canada) professor with the department of Chemistry at McGill University in Montreal Canada for 15 years prior to joining NCSU. Recent cross-appointments of his include affiliations as a Finland Distinguished Professor of Chemistry with the Department of Chemistry at the University of Helsinki in Finland and his visiting Distinguished Professorship with the Centre of Excellence for Advanced Materials Research, Jeddah. He is a Fellow of the Royal Society of Chemistry, Fellow of the International Academy of Wood Science and a Fellow of the Canadian Institute of Chemistry. He also serves as an editor and on the editorial boards of five scientific journals. He has served as the Division Chair and Secretary of the Cellulose and Renewable Materials of the American Chemical Society. The work of his group focuses on the organic chemistry of wood components and the development of novel analytical methods and new chemistries for transforming the carbon present in our trees toward producing valuable chemicals, materials, and energy.

Comparison of lignin and polyacrylonitrile precursors

sp^2/sp^3 hybridized carbon considerations

Lignin-derived CFs have been promoted as a sustainable, low-cost replacement to PAN-derived CFs. The performance of single component lignin-derived CFs has not come close to that of PAN-derived fibers, whereas CFs made from blends of lignin and other proven polymers, such as PAN, have come closer, but still require much improvement.[1] CFs derived from a mixture of lignin and PAN typically exhibit enhanced performance and graphitic structure relative to single component lignin CFs; the enhanced performance is due to the presence of PAN, not lignin.[1,9,10] Regardless of whether pure lignin or a polymer blend is used to produce CFs, most researchers assume some level of structural transformation of lignin from disordered sp^3-hybridized carbon to graphitic sp^2-hybridized carbon. However, this assumption is often made without proper validation through the appropriate analytical techniques, particularly XRD and Raman spectroscopy. Researchers often attribute the relatively poor performance of lignin-derived CFs on issues related to impurities in feedstock, improper fiber diameter and density, prevalence of defects, and non-homogeneity of spun fibers, to name a few.[1] An overlooked reason for poor performance is the lack of graphitic sp^2

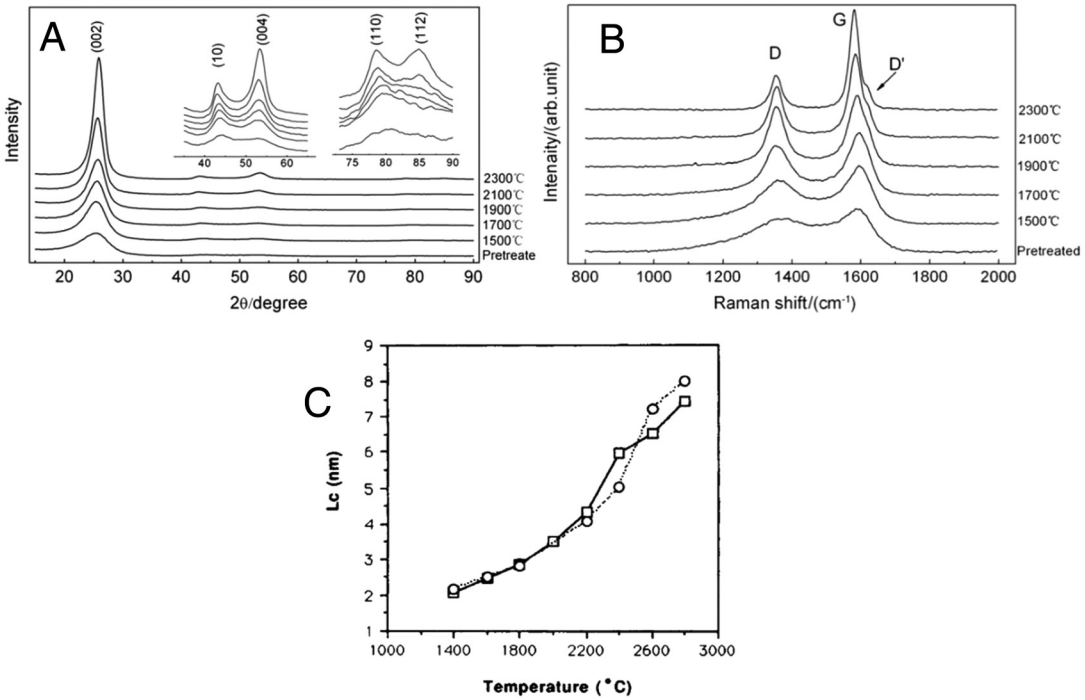

Fig. 2 (A) & (B): X-Ray diffractograms & Raman spectra of PAN-derived carbon fibers treated at different temperatures, respectively.[4] Reprinted with permission from Elsevier. Eqn (1) is the Scherer equation which shows an inverse relationship between peak width (B) of XRD diffractogram and graphitic crystallite size (L). Eqn (2) is the I_D/I_G ratio of Raman spectra intensity which is inversely related to graphitic crystallite size (L).[5,6] (C): Crystallite size (L_c) of PAN-derived carbon fibers graphitized at varying temperatures. Square: unmodified PAN precursor, Circle: PAN precursor modified with potassium permanganate.[7] Reprinted with permission from John Wiley & Sons.

hybridized structure in the final fiber product, especially for HMCFs. As early as 1951, various carbon precursors were extensively studied to determine the polymers best suited for forming graphite at elevated temperatures.[11] It was determined that polymers with heavily cross-linked, 3-dimensional structures are poorly suited for graphitization, whereas polymers with less cross-linking and more linear, 2-dimensional structures are better suited for graphitization.[11] The reactions that take place during the initial thermal stabilization stage of carbon fiber production significantly influence the degree of graphitization during later stages.[11] Polyacrylonitrile is a suitable precursor for high modulus carbon fibers due its linear, 2-dimensional polymeric chains that arrange themselves for cross-linking cyclization reactions during the initial thermal stabilization stage, as shown in Fig. 3;[8,12] the initial rearrangement and cyclization of PAN forms turbostratic structures suitable for graphitization at higher temperatures. It should be noted that high modulus, PAN-derived carbon fibers are not fibers of pure graphite, but rather fibers containing ribbon-like structures of ordered graphitic carbon interlocked with disordered domains of carbon.[13]

Chemical considerations

Natural lignin polymers are synthesized by plants to act as a resin providing strength to cellulose fibers, and therefore lignin is a relatively non-oriented material.[14,15] Lignins vary in their molecular configuration and reactivity due to differences in plant genetics and isolation methods. Researchers have used a multitude of different isolated lignins to produce CFs, although the mechanical properties of such CFs have generally been poor regardless of the plant species and isolation method used, relative to commercial CFs.[16–20] Three of the most common methods for isolating lignins include the use of organic solvents (organosolv, Alcell lignin), alkali solvents (kraft lignin), and pyrolysis (pyrolytic lignin).[18] Lignin obtained from the kraft process corresponds to ~85% of lignin removed in the pulping industry.[21] Among other advantages, high lignin extraction yield and less than 1–2% residual sulfur content make kraft lignin an abundant and relatively cheap carbon fiber precursor.[22] Extracted from lignocellulosic biomass using organic solvent extraction methods, organosolv lignin more closely resembles native lignin compared to kraft lignin. Compared to kraft lignin, organosolv and pyrolytic lignins require less purification and pretreatment steps prior to fiber spinning.[20] Kraft lignin is typically desalted using acid solutions prior to organic solvent purification to enhance thermoelastic properties and allow for effective spinning.[18,20] The industrial Lignoboost and Lignoforce processes that isolate lignin from kraft liquor *via* CO_2 precipitation provide a relatively pure lignin that requires fewer pretreatment steps.[23–25] Hosseinaei *et al.* compared the mechanical properties of CFs made from woody (hardwood) and non-woody (grass)-derived lignins using an organosolv isolation method.[16] The grass-derived lignins volatized thermally labile acid groups during

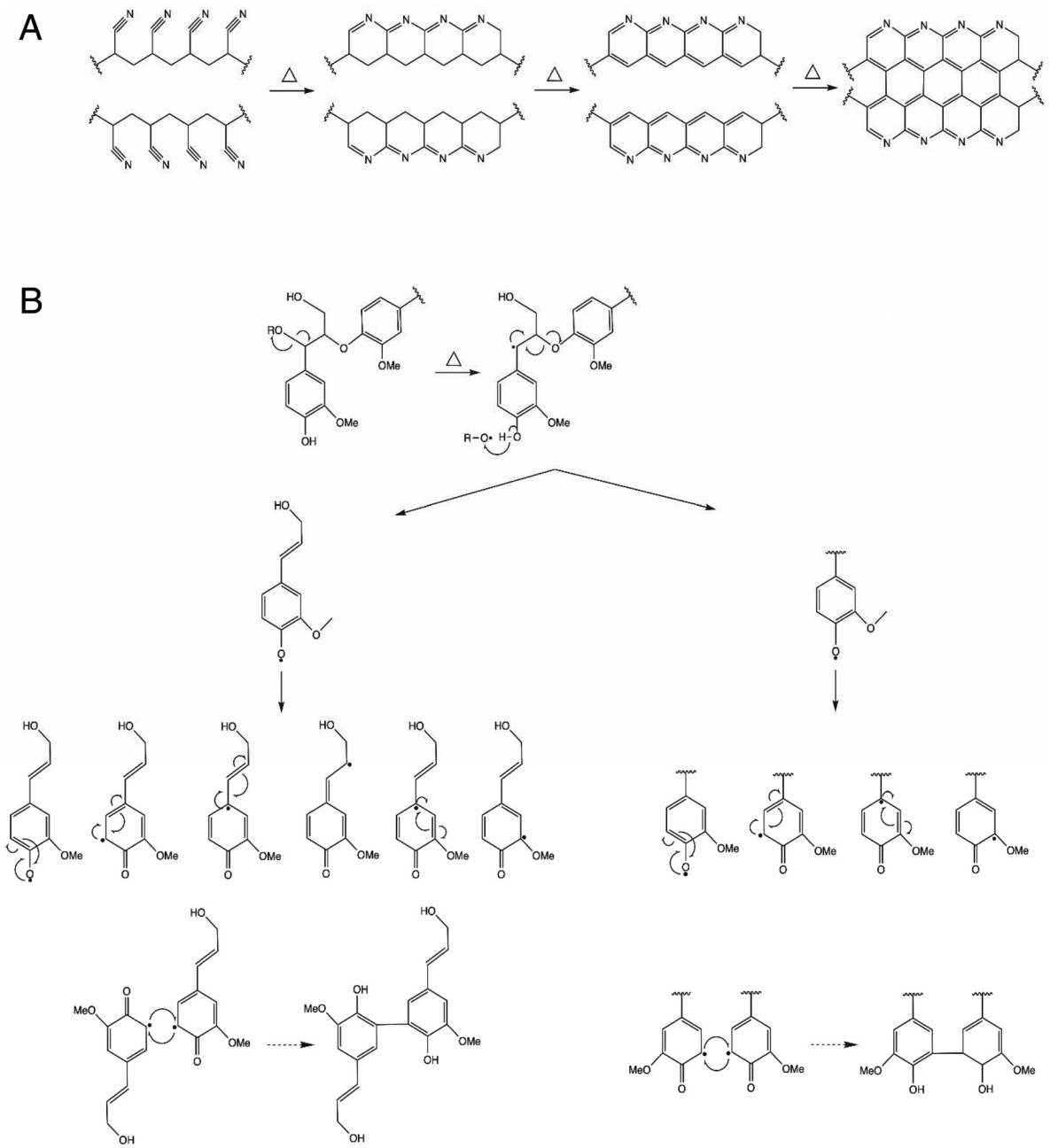

Fig. 3 (A) Cross-linking cyclization of PAN to form a 2-dimensional carbon lattice of graphitic structure.[8,12] (B) Cleavage of the β-O-4 linkage with free radical resonance enabling a multitude of pathways for radical coupling. Two examples of radical coupling to produce 5–5′ carbon–carbon bonds are provided.[28]

melt-spinning which led to defects in the CFs and ultimately poor strength, compared to the hard wood-derived lignins which were more stable. Although lignins from various plant species and isolation methods have been used for producing CFs, there is a general lack of consensus regarding which lignin type provides optimal CF properties. The lack of consensus is partly due to the large number of process variables when producing CFs, particularly during purification, pretreatment, spinning, and stabilization. Moreover, there has yet to be a published study in which the graphitic structures of CFs made from various lignin types were analyzed and compared.

Irrespective of the type of lignin, thermal treatment yields condensed structures, although the proportion of linkages varies with lignin type.[26–28] Thermal treatment of kraft lignin at relatively low temperatures creates phenoxy radical resonance structures that enable a multitude of coupling reactions, two of such are shown in Fig. 3.[28] The β-O-4 linkages present in kraft lignin give rise to two parallel reactions, one forming an enol ether[28,29] and the other forming phenoxy radicals

which result in condensed structures through radical coupling.[27,28] Molecular rotation is restricted due to formation of carbon–carbon bonds, which maintain molecular position.[21] As the temperature increases to ~500 °C during lignin carbonization, volatiles including H_2O, CO, CH_4 and CO_2 are liberated and oligomeric tars form on the surface of the carbon fibers.[30] Upon further increase in temperature, decomposition of side chains followed by aromatic condensation takes place. At 800–1000 °C, solid-state nuclear magnetic resonance and Fourier-transform infrared spectroscopy have been used to show some aromatic rings begin to rupture.[26,30] Zhang *et al.* proposed that these structures may further decompose and rearrange into non-graphitic, disordered domains during carbon fiber production.[30] However, there is no general consensus on the mechanisms involved in carbonization of lignin.

The regular structure of PAN coupled with the thermally induced elimination chemistry depicted in Fig. 3A provides a consistently homogeneous chemical pattern composed of a high number of sp^2 centers. However, when embarking from lignin, it becomes readily apparent that efforts to create such regular patterns, using the outlined limited mechanistic data, requires a lot more speculation for the creation of even a tenuous and unsubstantiated representation. While 5–5′ carbon–carbon bonds may form *via* the coupling of C5 carbon centered radicals originating from the phenoxy radicals shown in Fig. 3B, these may account for only but a fraction of the final structure. For lignin to become a regular carbonaceous material composed of a high number of sp^2 centers one needs additional documented detailed thermally induced coupling and elimination chemistry. One potential pathway for lignin graphitization is to induce the aforementioned chemistry *via* the installation of thermally reactive propargyl centers prior to high temperature thermal treatment as already exemplified by the effort of the Argyropoulos group.[31,32]

Numerous reactions take place during lignin carbonization, with the lack of uniform repeating units and abundance of irregular side chains promoting the development of disordered char. Therefore, the irregular, complex and variable structure of lignin likely inhibits rearrangement and cross-linking cyclization during carbonization—a necessity for highly graphitic carbon fibers. Nevertheless, many researchers assume lignin graphitizes similarly to PAN during carbon fiber production, even though the polymeric reactivity of PAN and lignin vary significantly during thermal treatment.

Temperature–strength relationship considerations

As shown in Fig. 4, the tensile modulus values for commercial PAN-derived CFs increase with temperature, as one would expect due to the development of graphitic crystallites along the fiber axes.[33,34] Researchers developing lignin-derived CFs use performance metrics of commercial CFs as benchmarks for further research and development. Given that the tensile modulus values of commercial CFs increase during high temperature treatment, one would expect the same from lignin-derived CFs; even if lignin-derived CFs have low starting modulus values relative to PAN, their modulus values should

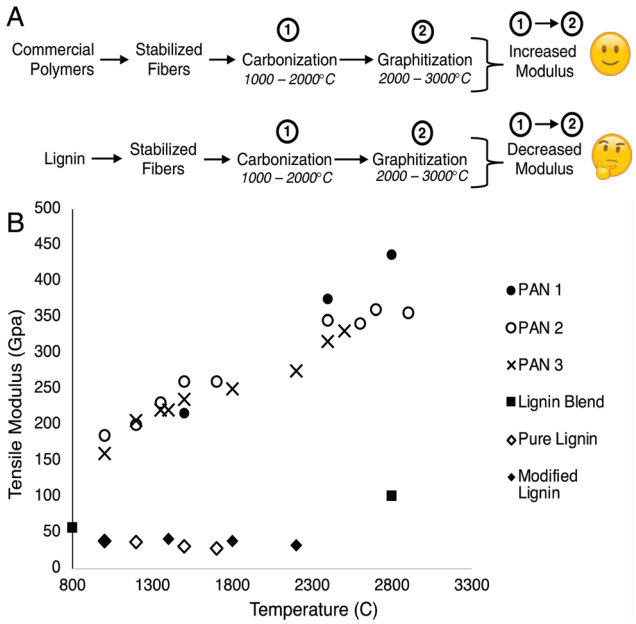

Fig. 4 (A) Schematic conveying an overlooked discrepancy in the temperature–modulus relationship among lignin-derived and commercial carbon fibers. (B) A plot showing the change in tensile modulus with respect to temperature for six carbon fibers (adapted from ref. 33–37). PAN 1, 2, & 3: Polyacrylonitrile carbon fibers treated at 1000–2900 °C,[33,34] Lignin Blend: Carbon fibers derived from pyrolysis fuel oil blended with hardwood kraft lignin treated at 800 and 2800 °C,[36] Pure Lignin: Carbon fibers derived from softwood kraft lignin treated at 1000–1700 °C,[35] Modified Lignin: Carbon fibers derived from acylated softwood lignin treated at 1000–2200 °C.[37]

still increase at higher temperatures. Interestingly, data from the literature indicate that the tensile modulus values of lignin-derived CFs either minimally increase, stay the same, or decrease with increasing temperature, as shown in Fig. 4.[35–37]

Unfortunately, the aforementioned statements regarding the lack of graphitic structure in lignin-derived CFs cannot be confidently validated due to a lack of published data showing evidence of such. However, there is an emerging field of research targeting the development of new methods to convert lignin and other bioresources into graphite for electrochemical applications, such as anodes for Li-ion batteries.[35,38–45] The lignin graphitization procedures used in these studies are similar to those used in carbon fiber studies, with the major exception being that strength properties are not optimized since electrode applications do not require such. Instead, lignin graphitization studies optimize for graphitic structure formation, and usually small graphitic particles are produced, not fibers.

Nevertheless, significant insight can be gained from comparing graphite quality reported in lignin graphitization studies to the sought after graphite quality of commercial CFs.

Graphitization of pure lignin

Highly graphitic structure has been claimed to be present in organosolv lignin-derived CFs treated up to 2700 °C, as shown

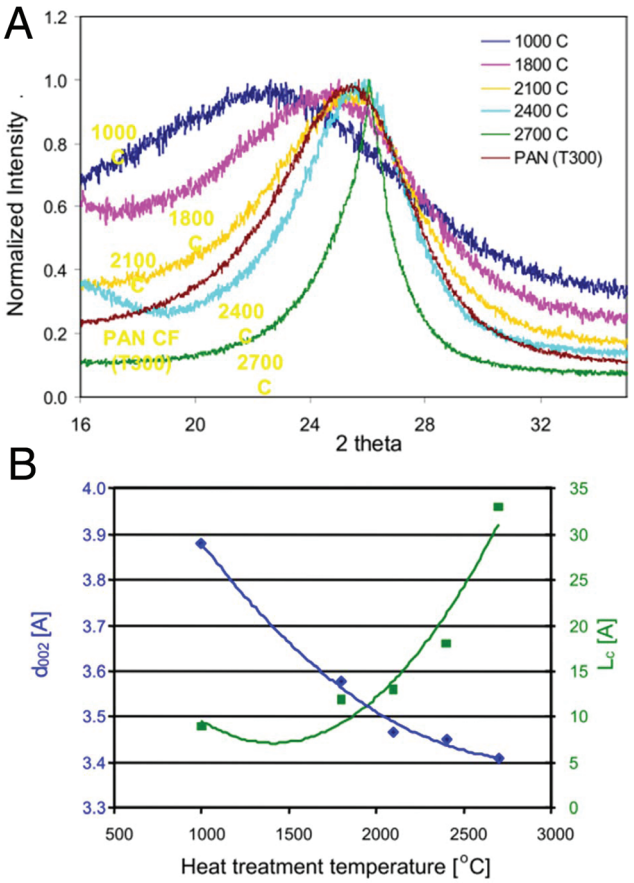

Fig. 5 (A) X-ray diffractograms of organosolv lignin-derived CFs treated at different temperatures. T300 represents Toray's commercial, baseline CF with a relatively low tensile modulus. (B) Interlayer spacing and crystallite size of organosolv lignin-derived CFs as determined by the XRD results.[18,46] Plots are from a publicly available presentation given by the US Dept. of Energy.[46]

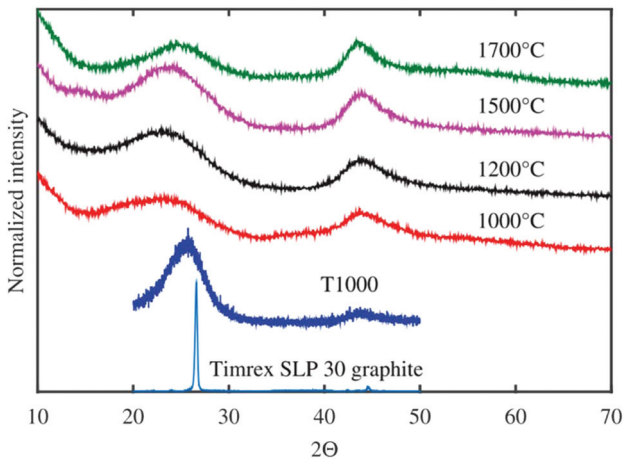

Fig. 6 XRD diffractograms with normalized intensities for kraft lignin-derived carbon fibers carbonized at varying temperatures. Timrex SLP 30 is a commercial graphite product and T1000 is a commercial, intermediate modulus PAN-derived carbon fiber.[35] Reprinted with permission from Walter De Gruyter & Company.

by the XRD diffractograms, graphitic crystallite sizes, and decreasing interlayer spacings in Fig. 5.[18,46] However, these studies found no increase in tensile modulus or other strength properties with increased treatment temperature, agreeing with the data provided in Fig. 4. This discrepancy means that lignin-derived CFs likely graphitize much differently than PAN-derived CFs, which is corroborated with XRD diffractograms of lignin- and PAN-derived CFs treated at 1800 °C; at 1800 °C, PAN-derived fibers are quite graphitic (Fig. 2A), while lignin-derived CFs are quite disordered (Fig. 5A). As shown in Fig. 5, the lignin-derived CFs do not show strong evidence of graphitic structure until 2700 °C; a jagged baseline, broad peak, and low intensity indicate disorder. The T300 PAN-derived CF used for comparison is Toray's commercialized baseline CF with a relatively low tensile modulus, and therefore it's not an ideal CF for comparison with the lignin-derived CFs treated at high temperatures;[47] the T300 PAN-derived CF is likely not produced at a high temperature, and therefore highly graphitic structure is not expected. As shown in Fig. 2, the degree of graphitization for PAN-derived carbon fibers is significantly dependent upon treatment temperature, and therefore the use of T300 for comparison is probably not valid. It would be helpful if high modulus PAN-derived CFs, such Toray's M40J, were used to compare graphitic structure with lignin-derived CFs treated at high temperatures. Nowak *et al.* (2018) recently published results on kraft lignin-derived carbon fibers for use in lithium-ion battery electrodes.[35] As shown in Fig. 6, the degree of graphitization is quite poor up to 1700 °C. The T1000 PAN-derived CF used for comparison is Toray's intermediate modulus CF, and therefore not an ideal CF for comparison with the lignin-derived CFs treated at high temperatures.[47] Tenhaeff *et al.* (2014) prepared organosolv lignin-derived carbon fibers for application in Li-ion battery anodes.[48] The CFs were carbonized at 1000, 1500, and 2000 °C. As shown in Fig. 7A, graphitic structure increased with temperature, however, the jagged baseline, low intensity, and wide peak indicate the degree of graphitization was less than that found in commercial, high modulus CFs. As shown in Fig. 7B, the I_D/I_G ratio of the Raman spectra for the CFs treated at 2000 °C appears to show stronger evidence of graphitic structure than its corresponding X-ray diffractogram. The reason for disagreement among XRD and Raman results might stem from the difference in detection mechanisms: XRD typically takes a bulk measurement of crystalline structure, whereas Raman measurements can vary from a single point to mapping of many points. A single point measurement *via* Raman that detects graphitic structure does not mean the entire material is graphitic, hence why large mapping should be done to avoid misleading results. Researchers should provide as much information as possible with regards to the method used for Raman spectroscopy. Garcia-Negron *et al.* (2017) (Fig. 8) prepared carbon materials from kraft lignin for use in energy storage applications.[42] The kraft lignin underwent an initial carbonization at 1000 °C under nitrogen gas,

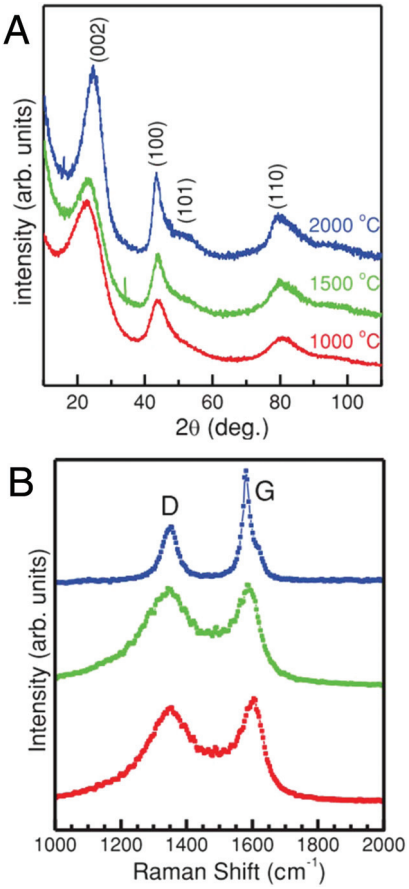

Fig. 7 (A) XRD diffractograms and (B) Raman spectra of organosolv-lignin derived carbon fibers carbonized at different temperatures.[48] Reprinted with permission from John Wiley & Sons.

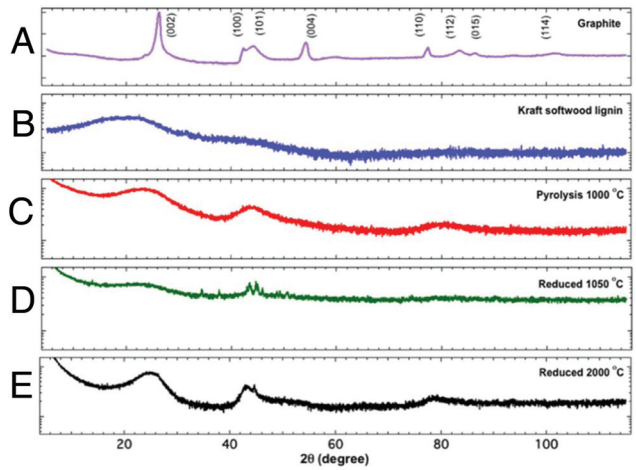

Fig. 8 XRD diffractograms of (A) graphite, (B) kraft lignin, (C) carbon fibers treated at 1000 °C under N_2, and carbon fibers treated at (D) 1050 °C and (E) 2000 °C under H_2.[42] Reprinted with permission from John Wiley & Sons.

followed by ball milling to reduce particle size to nanometer range, and then finally a thermal reduction treatment in which the carbonized powder was heated to 1050 and 2000 °C under hydrogen gas. As shown in Fig. 8, the graphitic structure resultant from high temperature treatment was minimal. Köhnke *et al.* (2018) successfully graphitized kraft lignin at 2000 °C, as shown in Fig. 9.[38] Interestingly, sulfite lignin graphitized to a much lesser extent than kraft lignin, underlining the importance of starting polymer structure and composition. Notably, Köhnke *et al.* used fine lignin powders resultant from spray-drying, with spherical diameters on the order of 1–6 microns. Multiple studies that successfully graphitized lignin used intensive milling or other techniques to reduce particle size to the micron level prior to thermal treatment, indicating that initial particle size may play a major role in the degree of graphitization.[38,40,49] Yoon *et al.* (2018) carbonized acid hydrolysis lignin at 900 and 1300 °C for use as anode material in a Na-ion battery.[43] As shown in Fig. 10, the characteristic (002) peak of graphite (2θ = 26.7°) is not detectable. The broad 002 peak indicates the existence of small graphitic domains present among the predominantly disordered carbon, but the total degree of graphitization is minimal. For comparison, X-ray diffractograms of PAN fibers carbonized at similar temperatures (1000–1500 °C) do show evidence of graphitic structure (Fig. 2A).

Ding *et al.* (2018) successfully isolated graphene quantum dots (GQDs) using alkali lignin as the feedstock.[50] The experimental procedure involved the partial depolymerization of alkali lignin *via* nitric acid treatment, followed with hydrothermal carbonization of the solids, and finally long-duration (1 week) dialysis of the solution resultant from hydrothermal carbonization to isolate water soluble GQDs. The authors were able to show graphitic structure in the quantum dots through the use of XRD, Raman spectroscopy, and ^{13}C cross-polarization magic angle spinning nuclear magnetic resonance (^{13}C CP MAS NMR). As shown in Fig. 11, the peak at 130 ppm indicates an abundance of fused SP^2 carbons which is characteristic of graphitic materials. Solid state NMR, such as ^{13}C CP MAS NMR, provides more structural granularity than XRD and Raman spectroscopy for complex solid materials like carbonized biomass, and therefore this technique should be used by researchers focused on lignin-derived carbon fibers. Researchers should however use caution when analyzing solid state NMR spectra of carbonized materials due to the likelihood of misinterpretation from anisotropic shielding and overlapping lineshapes. Ding *et al.*'s work suggests the use of hydrothermal carbonization might be an avenue towards higher quality carbon fibers *via* the enhanced development of graphitic structure. Chu *et al.* (2013) used ^{13}C NMR to analyze amorphous char materials generated from pyrolysis of a lignin model compound and proposed a mechanism that involves random repolymerization of radical species, thus corroborating points made in our aforementioned discussion on the disordered rearrangement of lignin during high temperature treatment (Fig. 3B).[51]

Overall, the literature shows graphitization of single component lignin carbon fibers and raw lignin samples *via* thermal treatment alone is difficult to achieve. Evidence of graphitic structure is generally weak for various lignin types

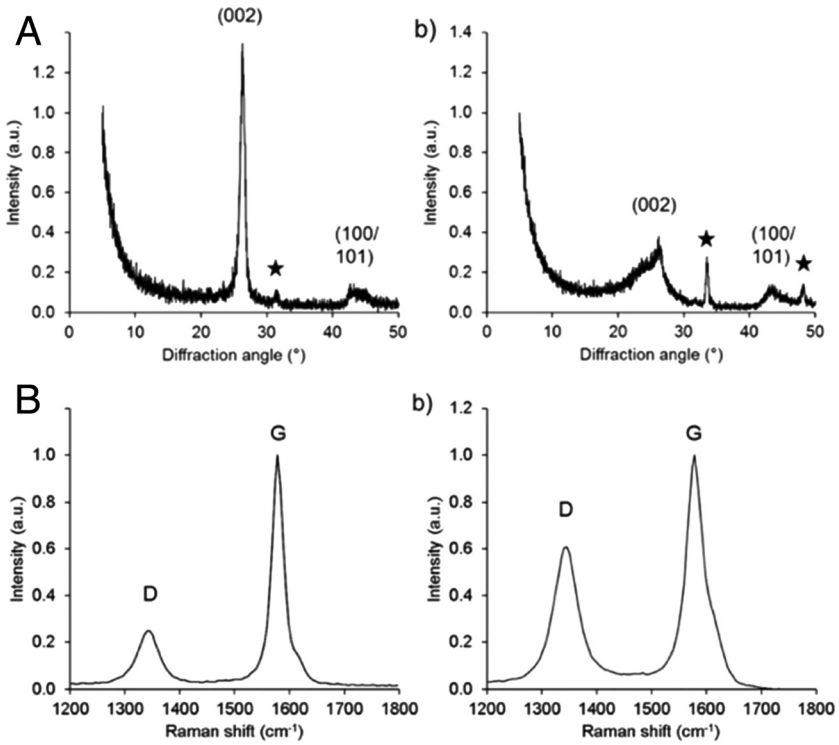

Fig. 9 (A) X-ray diffractograms and (B) Raman spectra of fine (1–6 μm) kraft lignin particles (left) and sulfite lignin particles (right) graphitized at 2000 °C.[38] Reprinted with permission from the American Chemical Society.

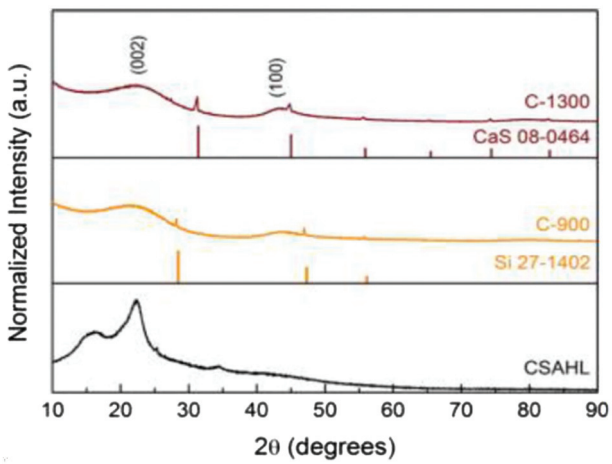

Fig. 10 X-ray diffractograms showing normalized intensity for acid hydrolysis lignin (CSAHL), CSAHL carbonized at 900 °C (C-900), and CSAHL carbonized at 1300 °C (C-1300).[43] Reprinted with permission from the American Chemical Society.

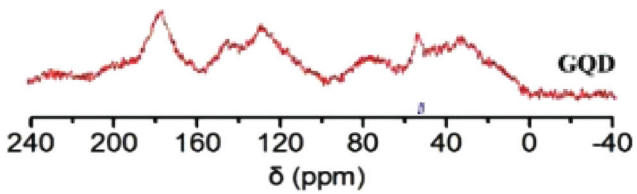

Fig. 11 ^{13}C cross-polarization magic angle spinning NMR of lignin-derived graphene quantum dots[50] Reprinted with permission from the Royal Society of Chemistry.

treated at temperatures ranging from 1000–2000 °C. There appears to be an improvement in graphitization when lignin particle size is significantly reduced prior to thermal treatment. The lack of clear evidence for graphitic structure in lignin-derived carbon fibers indicates the carbonization chemistry of such fibers differs quite significantly when compared to PAN-derived carbon fibers.

Graphitization of fractionated lignin

Jin *et al.* (2018) isolated and fractionated softwood kraft lignin from black liquor using the ALPHA process, which uses liquid–liquid equilibrium present in an acetic acid–water solution.[52] This method allows for separating lignin by molecular weight through adjusting the ratio of acetic acid to water. The researchers used this feature to produce lignin-derived CFs from three samples with different molecular weights, and they found that tensile strength and modulus increase as molecular weight increases. The improved carbon fiber performance is most likely due in part by the increased level of graphitic structure present in the higher molecular weight lignin-derived carbon fibers, as shown in Fig. 12; a decrease in I_D/I_G ratio corresponds to an increase in graphite crystallite size. Liu *et al.* (2018) extracted and fractionated lignin from corn stalk using differences in pH, and the resultant fractions were used as pre-

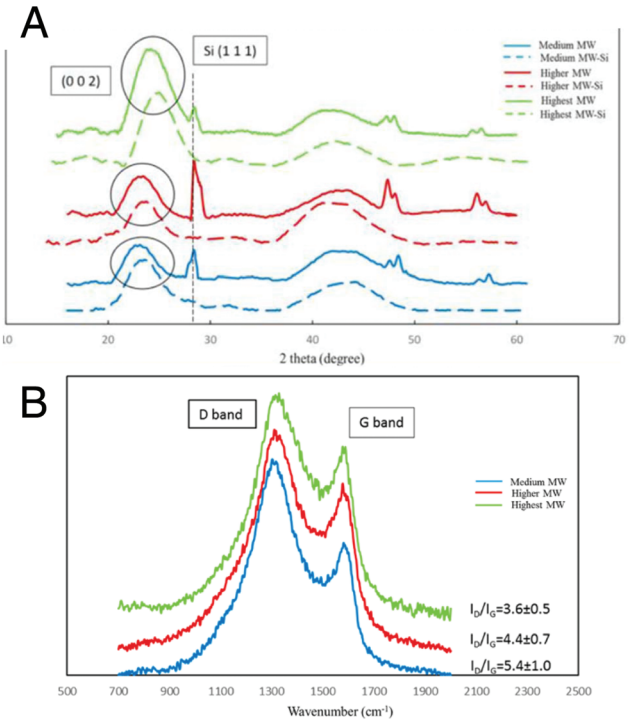

Fig. 12 (A) X-ray diffractograms and (B) Raman spectra of carbon fibers derived from lignins of varying molecular weight.[52] Molecular weight scale: Green – highest, red – intermediate, blue – lowest. Reprinted with permission from the American Chemical Society.

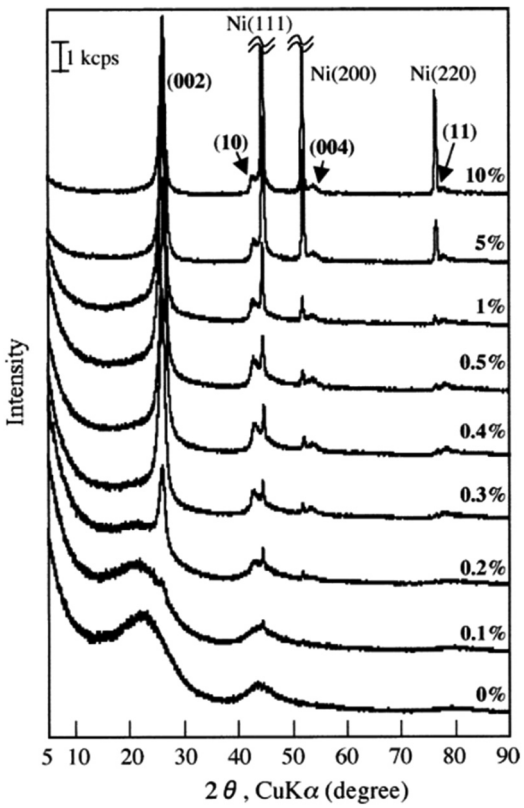

Fig. 13 X-ray diffractograms of acid hydrolysis lignin carbonized at 1000 °C with varying nickel catalyst loadings.[44] Reprinted with permission from Springer Japan.

cursors mixed with PAN (1 : 1 ratio) prior to carbonization.[55] High molecular weight lignin (M_w: 8170 g mol^{-1}) produced carbon fibers with an elastic modulus of 4.5 ± 0.1 GPa, compared to those produced from low molecular weight lignin (M_w: 4467 g mol^{-1}) which had an elastic modulus of 2.6 ± 0.4.[55] Also, Li *et al.* (2017) developed a method of lignin fractionation using an enzyme treatment and further dialysis to study the effect of molecular weight and polydispersity on the properties of lignin-PAN carbon fibers.[56,57] The elastic modulus values for all lignin-derived CFs increased with molecular weight. High molecular weight and low polydispersity enhances polymer uniformity and limits the formation of fiber defects during stabilization and carbonization.[52–54] Although higher molecular weight lignins were shown to enhance graphitic structure and improve performance, the mechanical properties were still inferior to those of PAN-derived CFs and thus the generalized observation of lignins' inability to graphitize persists. Treatment of fractioned lignins at higher temperatures might show a further increase in graphitic structure and thereby an increase in tensile moduli. Ideally, research into lignin-derived carbon fibers will continue to progress such that graphitic structure development can be achieved at relatively moderate temperatures (<1500 °C).

Catalytic graphitization of lignin

Most studies that attempt graphitization of lignin use furnaces with temperature limits around 1500 °C, and therefore transition metal catalysts are often used to obtain an improved graphitic structure. For example, Kubo *et al.* successfully graphitized acid hydrolysis lignin through the use of a nickel catalyst, as shown in Fig. 13.[44] The mechanism by which transition metals catalyze the conversion of disordered lignin to graphitic carbon is still under investigation, but there are two emerging theories: (1) dissolution of carbon into nanosized catalyst particles followed by graphitic layering and (2) near-eutectic liquid droplets of metal carbide formation and then decomposition upon high temperature treatment resulting in graphite.[58] As shown in Fig. 13, the degree of graphitization increases with catalyst loading. Neeli *et al.* (2018) conducted an interesting set of experiments in which they used iron to catalytically graphitize different fractions of lignocellulose, namely cellulose, hemicellulose, and lignin.[59] As shown in Fig. 14, essentially no graphitic structure was detected in lignin, whereas a moderate degree of graphitic structure was detected in hemicellulose and cellulose. The ability of cellulose to graphitize is not surprising since Rayon, a cellulose derivative, is a proven precursor for the production of carbon fibers.[1] However, the inability of lignin to graphitize is surprising given the extensive research done on lignin-derived CFs. Yan *et al.* (2018) investigated the effect different gases have on the formation of graphitic structure during catalytic graphitization of kraft lignin at 1000 °C.[60] Methane and natural gas in

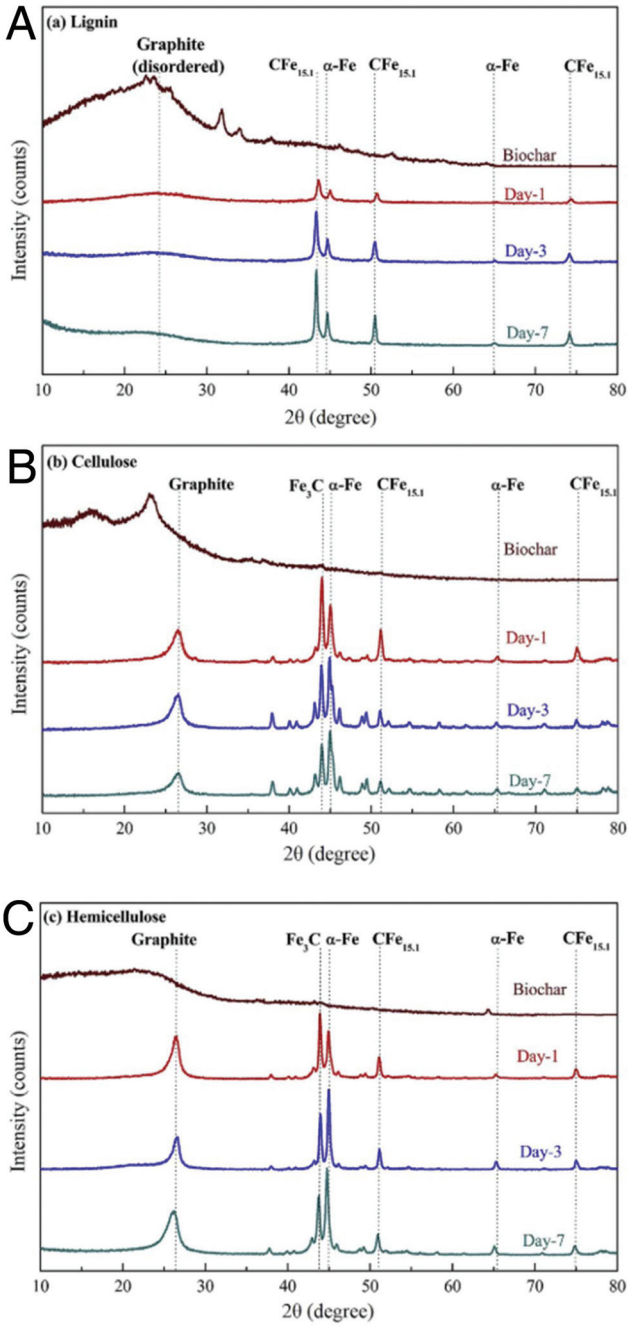

Fig. 14 XRD diffractograms of iron catalyzed biomass fractions carbonized at 1000 °C (A) lignin, (B) cellulose, and (C) hemicellulose. Top diffractograms represent hydrochar samples prior to iron catalyzed pyrolysis. Day-1, 3, 7 refer to the number of days the iron impregnated hydrochar samples were left to dry in a 110 °C oven prior to pyrolysis.[59] Reprinted with permission from Elsevier.

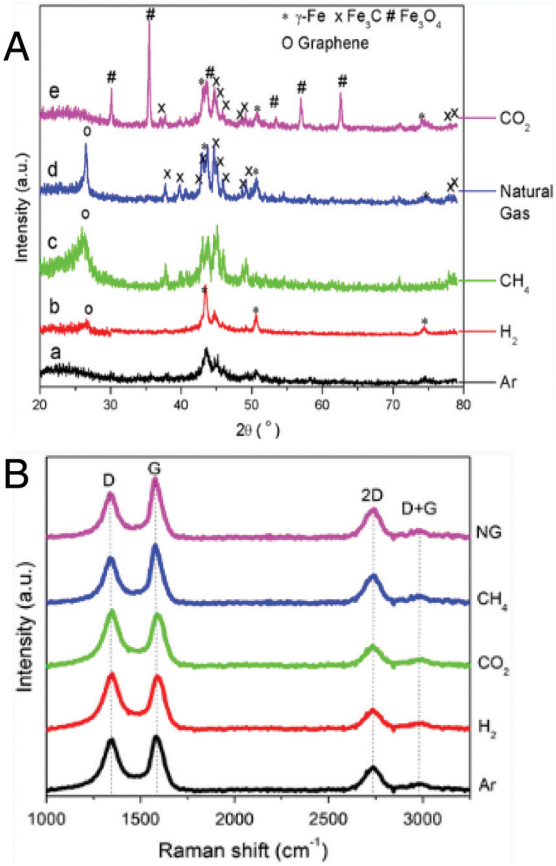

Fig. 15 (A) XRD diffractograms and (B) Raman spectra for iron catalyzed kraft lignin at 1000 °C under varying gases.[60] Reprinted with permission from Springer Nature.

the ambient gas phase were found to improve graphitic structure development, and hydrogen and carbon dioxide were found to have an etching effect on solid carbon species. The improved graphitic structure from natural gas and methane might be due to vapor deposition on the metal catalysts and subsequent graphitization. As shown in Fig. 15, the X-ray diffractograms for kraft lignin carbonized under inert gases show poor graphitic structure development. Banek *et al.* (2018) recently developed an innovative method to catalytically graphitize multiple biomass resources, including whole biomass, cellulose, and lignin.[40] Their method involves vigorously ball milling a mixture of iron and lignin prior to a 2-step graphitization procedure: step 1 involves carbonization under nitrogen at 600 °C for 30 minutes and step 2 involves laser irradiation to induce graphitization. As shown in Fig. 16, Banek *et al.* achieved highly graphitic structure for all of the biomass resources tested; interestingly, wood flour and cellulose resulted in better graphitic structure than lignin. Similar to Köhnke *et al.*'s work,[38] Banek *et al.* started with lignin of very small particle size. Garcia-Negron *et al.* also used small particles for high temperature graphitization,[42] but obtained less graphitic materials than Köhnke and Banek. One possible reason for the discrepancy in results among the papers is that Köhnke and Banek reduced the particle size of raw lignin prior to any thermal treatment, whereas Garcia-Negron reduced particle size after an initial carbonization at 1000 °C. Therefore, the use of small (1–50 μm) untreated lignin particles seems advantageous for subsequent graphitic structure development and warrants serious attention.

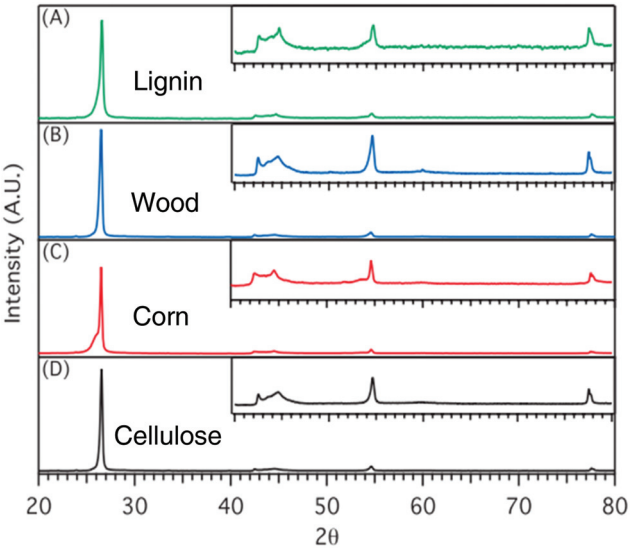

Fig. 16 XRD diffractograms of (A) lignin, (B) wood flour, (C) corn cob, and (D) cellulose catalytically graphitized *via* a 2-step procedure involving carbonization at 600 °C and laser irradiation.[40] Reprinted with permission from the American Chemical Society.

Several researchers have catalytically graphitized carbon nanotubes on the surface of PAN-derived CFs *via* chemical vapor deposition (CVD) to improve performance properties such as thermal stability and electrical conductivity, however, there has been little investigation into using such a technique on lignin-derived CFs.[61–64] Xu *et al.* (2014) decorated the surface of CFs derived from a mixture of lignin and PAN with carbon nanotubes to enhance thermal stability.[61] The carbon nanotubes were synthesized on the surface of the fibers *via* CVD using iron and palladium nanoparticles, and electron energy loss spectroscopy (EELS) was used to identify both amorphous and graphitic regions. Like solid state NMR, EELS is a powerful analytical tool that should be used more often by researchers focused on developing lignin-derived carbon fibers. Li *et al.* (2014) and Tang *et al.* (2012) also used EELS to quantify the sp^2 content and C–C bond lengths of bio-based graphene quantum dots thereby providing robust support to their hypotheses.[65,66]

Innovative techniques have been developed to decorate CF surfaces with graphitic carbon nanotubes, but there has been a lack of innovation in incorporating higher levels of graphitic domains within the bulk of fibers. Given that PAN-derived CFs possess graphitic domains within fibers and not only on their surfaces, researchers should use the aforementioned studies on catalytic graphitization to innovate new methods for enhancing graphitic structure throughout the bulk of lignin-derived CFs, but without hindering strength properties. The use of transition metals to catalyze the conversion of lignin to graphite has been primarily used for electrochemical applications, such as electrodes; however, the method might benefit researchers interested in high modulus lignin-derived carbon fibers. Catalysts significantly increase graphitic structure development during lignin carbonization, and therefore an opportunity exists to increase carbon fiber strength if utilized in an innovative fashion. Given that the catalytic mechanism is still under investigation, there is uncertainty in how fiber strength properties will be affected by the presence of metals. In addition, the removal of metals post-thermal treatment would likely require strong acid washing of the fibers, which might negatively affect strength properties. Nonetheless, doping lignin with transition metals prior to carbon fiber production is an intriguing avenue for further research.

Conclusions

The use of lignin for high modulus carbon fibers may be fundamentally impaired due to the poor ability of lignin to graphitize, relative to PAN and other commercial polymers. The amount of robust evidence supporting the claim that lignins graphitize similarly to PAN at high temperatures is minimal and must be expanded through the use of proper analytical techniques such as X-ray diffraction and Raman spectroscopy. Although X-ray diffraction and Raman spectroscopy are capable of evaluating the crystalline domains of graphitic carbon materials, their ability to evaluate molecular configurations present in disordered domains is weak. The complex transformations of lignin during graphitization result in ordered domains inter-mixed with disordered domains, thereby warranting the use of additional techniques that can evaluate particular molecular configurations present in the disordered domains. Solid-state nuclear magnetic resonance and electron energy loss spectroscopy have been used by other researchers to determine the molecular configurations of disordered domains in activated carbons and related biochar materials, but the techniques have been underutilized on lignin-derived graphitic materials.[67,68] We recommend relevant research efforts to focus on understanding the development of graphitic (ordered) and amorphous (disordered) domains of carbon fibers *via* X-ray diffraction, Raman spectroscopy, solid-state nuclear magnetic resonance, and electron energy loss spectroscopy.

The literature shows lignin-derived carbon fiber tensile modulus values do not increase with treatment temperature in the same manner as PAN (Fig. 4). We propose the poor ability of lignins to graphitize is the primary cause for this discrepancy, and we provide evidence from multiple studies aimed at producing graphite from lignin. Some researchers have successfully demonstrated the graphitization of various lignins through the use of small particle sizes, molecular weight fractions, and transition metal catalysts. Transition metal catalysts appear to provide highly graphitic structure at relatively low temperatures, but the applicability of these catalysts to lignin carbon fiber production may be limited. Nonetheless, the use of metal catalysts for lignin-derived, high modulus carbon fibers warrants attention. In addition, the effects of lignin particle size and molecular weight on graphitization and the resultant carbon fiber strength should be investigated further.

Author contributions

D. S. A. and W. J. S. conceived the critical review; D. S. A., W. J. S., S. P., D. B., and S. A. contributed to the introduction; D. S. A., W. J. S., A. J., and M. K. contributed to understanding the chemistry involved in lignin and PAN carbonization; W. J. S. & D. B. contributed to the section on pure lignin graphitization; A. S. contributed to the section on graphitization of fractionated lignin; W. J. S. and S. A. contributed to the section on catalytic graphitization; W. J. S. wrote the paper with input from all authors; D. S. A. made final edits to the paper.

Conflicts of interest

There are no conflicts to declare.

Acknowledgements

We thank all the publishers, journals, and authors who gave us permission to reprint figures and data for our critical review. This work was inspired by Dr. Argyropoulos' involvement in B-LigZymes project funded from the European Union's Horizon 2020 Research and Innovation programme under the Marie Sklodowska-Curie grant agreement No. 824017.

Notes and references

1 H. Brünig, D. Fischer, M. Al Aiti, G. Heinrich and D. Jehnichen, *Prog. Mater. Sci.*, 2018, **98**, 477–551.
2 W. Fang, S. Yang, X.-L. Wang, T.-Q. Yuan and R.-C. Sun, *Green Chem.*, 2017, **19**, 1794–1827.
3 X. Huang, *Materials*, 2009, **2**, 2369–2403.
4 A. Gao, C. Su, S. Luo, Y. Tong and L. Xu, *J. Phys. Chem. Solids*, 2011, **72**, 1159–1164.
5 S. Speakman, *MIT Cent. Mater. Sci. Eng*, 2015, 1–66.
6 A. C. Ferrari, *Solid State Commun.*, 2007, **143**, 47–57.
7 T. H. Ko, *J. Appl. Polym. Sci.*, 1996, **59**, 577–580.
8 C. D. Warren, *Carbon Fiber Precursors and Conversion*, 2016, https://www.energy.gov/sites/prod/files/2016/09/f33/fcto_h2_storage_700bar_workshop_3_warren.pdf.
9 J. Jin and A. A. Ogale, *J. Appl. Polym. Sci.*, 2018, **135**, 1–9.
10 Q. Li, S. Xie, W. K. Serem, M. T. Naik, L. Liu and J. S. Yuan, *Green Chem.*, 2017, **19**, 1628–1634.
11 R. E. Franklin, *Proc. R. Soc. A*, 1951, **209**, 196–218.
12 M. S. A. Rahaman, A. F. Ismail and A. Mustafa, *Polym. Degrad. Stab.*, 2007, **92**, 1421–1432.
13 D. Li, C. Lu, S. Du, G. Wu, Y. Yang and L. Wang, *Appl. Phys. A: Mater. Sci. Process.*, 2016, **122**, 1–10.
14 L. Salmén, A. M. Olsson, J. S. Stevanic, J. Simonovic and K. Radotic, *BioResources*, 2012, **7**, 521–532.
15 C. Crestini, H. Lange, M. Sette and D. S. Argyropoulos, *Green Chem.*, 2017, **19**, 4104–4121.
16 O. Hosseinaei, D. P. Harper, J. J. Bozell and T. G. Rials, *ACS Sustainable Chem. Eng.*, 2016, **4**, 5785–5798.
17 Q. Yu, A. Bahi and F. Ko, *Macromol. Mater. Eng.*, 2015, **300**, 1023–1032.
18 D. A. Baker and T. G. Rials, *J. Appl. Polym. Sci.*, 2013, **130**, 713–728.
19 J. M. Rosas, R. Berenguer, M. J. Valero-Romero, J. Rodriguez-Mirasol and T. Cordero, *Front. Mater.*, 2014, **1**, 1–17.
20 W. Qin and J. F. Kadla, *J. Appl. Polym. Sci.*, 2012, **126**, 203–212.
21 F. Souto, V. Calado and N. Pereira, *Mater. Res. Express*, 2018, **5**, 1–30.
22 S. Laurichesse and L. Avérous, *Prog. Polym. Sci.*, 2014, **39**, 1266–1290.
23 L. Kouisni, P. Holt-Hindle, K. Maki and M. Paleologou, *Pulp Pap. Can.*, 2014, **115**, 18–22.
24 P. Tomani, *Cellul. Chem. Technol.*, 2010, **44**, 53–58.
25 Y. Nordström, I. Norberg, E. Sjöholm and R. Drougge, *J. Appl. Polym. Sci.*, 2013, **129**, 1274–1279.
26 M. Foston, G. A. Nunnery, X. Meng, Q. Sun, F. S. Baker and A. Ragauskas, *Carbon*, 2013, **52**, 65–73.
27 Q. Sun, R. Khunsupat, K. Akato, J. Tao, N. Labbé, N. C. Gallego, J. J. Bozell, T. G. Rials, G. A. Tuskan, T. J. Tschaplinski, A. K. Naskar, Y. Pu and A. J. Ragauskas, *Green Chem.*, 2016, **18**, 5015–5024.
28 C. Cui, H. Sadeghifar, S. Sen and D. S. Argyropoulos, *BioResources*, 2013, **8**, 864–886.
29 I. Norberg, Y. Nordström, R. Drougge, G. Gellerstedt and E. Sjöholm, *J. Appl. Polym. Sci.*, 2013, **128**, 3824–3830.
30 X. Zhang, Q. Yan, W. Leng, J. Li, J. Zhang, Z. Cai and E. B. Hassan, *Materials*, 2017, **10**, 1–15.
31 S. Sen, H. Sadeghifar and D. S. Argyropoulos, *Biomacromolecules*, 2013, **14**, 3399–3408.
32 H. Sadeghifar, S. Sen, S. V. Patil and D. S. Argyropoulos, *ACS Sustainable Chem. Eng.*, 2016, **4**, 5230–5237.
33 E. Fitzer and L. M. Manocha, *Carbon reinforcements and carbon/carbon composites*, Springer-Verlag, Berlin Heidelberg, 1998.
34 A. Galiguzov, A. Malakho, V. Kulakov, A. Kenigfest, E. Kramarenko and V. Avdeev, *Carbon Lett.*, 2013, **14**, 22–26.
35 A. P. Nowak, J. Hagberg, S. Leijonmarck, H. Schweinebarth, D. Baker, A. Uhlin, P. Tomani and G. Lindbergh, *Holzforschung*, 2018, **72**, 81–90.
36 M. S. Kim, D. H. Lee, C. H. Kim, Y. J. Lee, J. Y. Hwang, C. M. Yang, Y. A. Kim and K. S. Yang, *Carbon*, 2015, **85**, 194–200.
37 L. M. Steudle, E. Frank, A. Ota, U. Hageroth, S. Henzler, W. Schuler, R. Neupert and M. R. Buchmeiser, *Macromol. Mater. Eng.*, 2017, **302**, 1–11.
38 J. Köhnke, H. Rennhofer, H. Lichtenegger, A. Raj Mahendran, C. Unterweger, B. Prats-Mateu, N. Gierlinger, E. Schwaiger, A.-K. Mahler, A. Potthast and W. Gindl-Altmutter, *ACS Sustainable Chem. Eng.*, 2018, **6**, 3385–3391.

39 D. Yoon, J. Hwang, W. Chang and J. Kim, *ACS Appl. Mater. Interfaces*, 2018, **10**, 569–581.
40 N. A. Banek, D. T. Abele, K. R. McKenzie and M. J. Wagner, *ACS Sustainable Chem. Eng.*, 2018, **6**, 13199–13207.
41 H. Qin, Y. Zhou, J. Huang, C. Zhang, B. Wang and S. Jin, *Int. J. Electrochem. Sci.*, 2017, **12**, 10599–10604.
42 V. Garcia-Negron, N. D. Phillip, J. Li, C. Daniel, D. Wood, D. J. Keffer, O. Rios and D. P. Harper, *Energy Technol.*, 2017, **5**, 1311–1321.
43 D. Yoon, J. Hwang, W. Chang and J. Kim, *ACS Appl. Mater. Interfaces*, 2018, **10**, 569–581.
44 S. Kubo, Y. Uraki and Y. Sano, *J. Wood Sci.*, 2003, **49**, 188–192.
45 M. Demir, Z. Kahveci, B. Aksoy, N. K. R. Palapati, A. Subramanian, H. T. Cullinan, H. M. El-kaderi, C. T. Harris and R. B. Gupta, *Ind. Eng. Chem. Res.*, 2015, **54**, 10731–10739.
46 F. S. Baker, *Low Cost Carbon Fiber From Renewable Resources*, 2010, https://www1.eere.energy.gov/vehiclesandfuels/pdfs/merit_review_2010/lightweight_materials/lm005_baker_2010_o.pdf.
47 Toray Carbon Fibers America Inc., Technical data sheet, https://www.toray.us/products/prod_004.html.
48 W. E. Tenhaeff, O. Rios, K. More and M. A. McGuire, *Adv. Funct. Mater.*, 2014, **24**, 86–94.
49 X. Zhao, Y. Yao, A. E. George, R. A. Dunlap and M. N. Obrovac, *J. Electrochem. Soc.*, 2016, **163**, A858–A866.
50 Z. Ding, F. Li, J. Wen, X. Wang and R. Sun, *Green Chem.*, 2018, **20**, 1383–1390.
51 S. Chu, A. V. Subrahmanyam and G. W. Huber, *Green Chem.*, 2013, **15**, 125–136.
52 J. Jin, J. Ding, A. Klett, M. C. Thies and A. A. Ogale, *ACS Sustainable Chem. Eng.*, 2018, **6**, 14135–14142.
53 E. Frank, F. Hermanutz and M. R. Buchmeiser, *Macromol. Mater. Eng.*, 2012, **297**, 493–501.
54 D. A. Baker, N. C. Gallego and F. S. Baker, *J. Appl. Polym. Sci.*, 2012, **124**, 227–234.
55 H. Liu, Z. Dai, Q. Cao, X. Shi, X. Wang, H. Li, Y. Han, Y. Li and J. Zhou, *ACS Sustainable Chem. Eng.*, 2018, **6**, 8554–8562.
56 Q. Li, S. Xie, W. K. Serem, M. T. Naik, L. Liu and J. S. Yuan, *Green Chem.*, 2017, **19**, 1628–1634.
57 Q. Li, W. K. Serem, W. Dai, Y. Yue, M. T. Naik, S. Xie, P. Karki, L. Liu, H. J. Sue, H. Liang, F. Zhou and J. S. Yuan, *J. Mater. Chem. A*, 2017, **5**, 12740–12746.
58 A. Gomez-Martin, J. Martinez-Fernandez, M. Ruttert, A. Heckmann, M. Winter, T. Placke and J. Ramirez-Rico, *ChemSusChem*, 2018, **11**, 2776–2787.
59 S. T. Neeli and H. Ramsurn, *Carbon*, 2018, **134**, 480–490.
60 Q. Yan, X. Zhang, J. Li, E. B. Hassan, C. Wang, J. Zhang and Z. Cai, *J. Mater. Sci.*, 2018, **53**, 8020–8029.
61 X. Xu, J. Zhou, L. Jiang, G. Lubineau, S. A. Payne and D. Gutschmidt, *Carbon*, 2014, **80**, 91–102.
62 S. A. Steiner, R. Li and B. L. Wardle, *ACS Appl. Mater. Interfaces*, 2013, **5**, 4892–4903.
63 K. J. Kim, J. Kim, W. R. Yu, J. H. Youk and J. Lee, *Carbon*, 2013, **54**, 258–267.
64 F. J. Garcia-Mateos, T. Cordero-Lanzac, R. Berenguer, E. Morallon, D. Cazorla-Amoros, J. Rodriguez-Mirasol and T. Cordero, *Appl. Catal., B*, 2017, **211**, 18–30.
65 X. Li, S. P. Lau, L. Tang, R. Ji and P. Yang, *Nanoscale*, 2014, **6**, 5323–5328.
66 L. Tang, R. Ji, X. Cao, J. Lin, H. Jiang, X. Li, K. S. Teng, C. M. Luk, S. Zeng, J. Hao and S. P. Lau, *ACS Nano*, 2012, **6**, 5102–5110.
67 X. Cao and K. Schmidt-Rohr, *Environ. Sci. Technol. Lett.*, 2018, **5**, 476–480.
68 C. E. Brewer, K. Schmidt-Rohr, J. A. Satiro and R. C. Brown, *AIChE J.*, 2010, **28**, 386–396.